



HAL
open science

Large second-harmonic generation of thermally poled sodium borophosphate glasses

Marc Dussauze, Evelyne Fargin, Michel Lahaye, Vincent Rodriguez, Frédéric Adamietz

► **To cite this version:**

Marc Dussauze, Evelyne Fargin, Michel Lahaye, Vincent Rodriguez, Frédéric Adamietz. Large second-harmonic generation of thermally poled sodium borophosphate glasses. *Optics Express*, 2005, 13 (11), pp.4064-4069. 10.1364/OPEX.13.004064 . hal-00019287

HAL Id: hal-00019287

<https://hal.science/hal-00019287>

Submitted on 13 Feb 2024

HAL is a multi-disciplinary open access archive for the deposit and dissemination of scientific research documents, whether they are published or not. The documents may come from teaching and research institutions in France or abroad, or from public or private research centers.

L'archive ouverte pluridisciplinaire **HAL**, est destinée au dépôt et à la diffusion de documents scientifiques de niveau recherche, publiés ou non, émanant des établissements d'enseignement et de recherche français ou étrangers, des laboratoires publics ou privés.

Large second-harmonic generation of thermally poled sodium borophosphate glasses

Marc Dussauze, Evelyne Fargin and Michel Lahaye

Institut de Chimie de la Matière Condensée de Bordeaux - UPR 9048 CNRS
Chateau Brivazac, Avenue du Dr. Schweitzer, 33608 Pessac Cedex, France.
dussauze@icmcb-bordeaux.cnrs.fr

Vincent Rodriguez and Frédéric Adamietz

Laboratoire de Physico-Chimie Moléculaire, UMR 5803 CNRS, Université Bordeaux I
351 cours de la Libération, 33405 Talence Cedex, France.
v.rodriguez@lpcm.u-bordeaux1.fr

Abstract: Second harmonic generation (SHG) has been obtained in a rich in sodium niobium borophosphate glass by a thermal poling treatment. The thermally poled glass SHG signal has been studied through an original analysis of both transmitted and reflected polarized Maker-fringe patterns. Therefore, the second order nonlinear optical (NLO) efficiency was estimated from the simulation of the Maker-fringe patterns with a stepwise decreasing profile from the anode surface. A reproducible $\chi^{(2)}$ susceptibility value as high as 5.0 ± 0.3 pm/V was achieved at the anode side. The nonlinear layer, found to be sodium-depleted up to 5 μm deep inside the anode side, identical to the simulated nonlinear zone thickness, indicates a complex space-charge-migration/nonlinear glass matrix response process.

© 2005 Optical Society of America.

OCIS codes: (160.2750) Glass and other amorphous materials; (190.4400) Nonlinear optics, materials; (160.4330) Nonlinear optical materials.

References and links

1. R.A. Myers, N. Mukherjee and S.R.J. Brueck, "Large second-order nonlinearity in poled fused silica," *Opt. Lett.* **16**, 1732 (1991).
 2. N. Mukherjee, R.A. Myers and S.R.J. Brueck, "Dynamics of second-harmonic generation in fused silica," *J. Opt. Soc. Am. B* **11**, 665 (1994).
 3. K. Tanaka, A. Narazaki, K. Hirao, "Surface structure and second order nonlinear optical properties of thermally poled $\text{WO}_3\text{-TeO}_2$ glasses doped with Na" *J. Opt. Soc. Am. B* **19**, 54-62 (2002).
 4. M. Guignard, V. Nazabal, J. Troles, F. Smektala, H. Zeghlache, Y. Quiquempois, A. Kudlinski, G. Martinelli, "Second-harmonic generation of thermally poled chalcogenide glass," *Optics Express* **13**, 789-795 (2005)
<http://www.opticsexpress.org/abstract.cfm?URI=OPEX-13-3-789>
 5. V. Rodriguez and C. Sourisseau, "General Maker-fringe ellipsometric analyses in multilayer nonlinear and linear anisotropic optical media," *J. Opt. Soc. Am. B* **19**, 2650 (2002).
 6. Y. Quimquempois, N. Godbout and S. Lacroix, "Model of charge migration during thermal poling in silica glasses Evidence of a voltage threshold for the onset of a second-order nonlinearity," *Phys. Rev. A* **65**, 43816 (2002).
 7. T. Cardinal, E. Fargin, G. Le Flem and S. Leboiteux, "Correlations between structural properties of $\text{Nb}_2\text{O}_5\text{-NaPO}_3\text{-Na}_2\text{B}_4\text{O}_7$ glasses and non-linear optical activities," *J. of Non Crist. Sol.* **222**, 228 (1997).
 8. T. Cardinal, E. Fargin, G. Le Flem *et al.*, "Nonlinear optical properties of some niobium(V) oxide glasses," *Eur. J. Solid State Inorg. Chem.* **t. 33**, 597 (1996).
 9. P. Thamboon, D. M. Krol, "Second-order nonlinearities in thermally poled phosphate glasses," *J. Appl. Phys.* **93**, 32-37 (2003).
-

1. Introduction

The development of optical communication technologies has created an important interest in materials with nonlinear optical properties. The ideal material should combine large nonlinear coefficients, good optical quality and low optical loss. It is now well known that in glasses a thermal poling treatment may induce a second-harmonic response suitable for electro-optical applications. Myers et al. have proposed a model where the $\chi^{(2)}$ signal induced by the thermal poling process may originate either from: 1) a third order non linear process through the remaining internal electric field (E_{int}), efficient in a layer of a few micrometers under the surface in contact with the anode or 2) the extent of a structural reorganization of hyperpolarizable entities [1, 2]. The best results were obtained in glasses with high $\chi^{(3)}$ coefficients. Tanaka [3] reported 2.2pm/V in WO_3 - TeO_2 glasses, but the induced signal is not stable in time. Recently, Guignard [4] obtained 4.4pm/V in a chalcogenide glass for applications in the IR spectral region. In this paper we report promising results obtained from a thermally poled sodium borophosphate niobium oxide glass.

2. Experimental conditions

2.1. Glass synthesis and characterization

Bulk samples with the same composition $Na_{10}P_{8.5}B_{1.5}Nb_{15}O_{65}$ were elaborated by a classical solid phase process. High purity reagent powders of $NaPO_3$, $Na_2B_4O_7$ and Nb_2O_5 were mixed and grounded, poured in a platinum crucible and melted at a temperature of 1300°C. The melt was quenched in a brass pre-form (1mm depth). The glass formed was annealed under air, 30°C under the glass transition temperature. Transparent samples 500 μ m thick were cut and polished on both sides.

Energy Dispersive X-Ray spectroscopy (EDS) allowed the identification of the elemental composition of the studied samples, imaged with a Scanning Electron Microscope (SEM), which permitted to control the stoichiometry of the glasses.

2.2. Optimization of temperature and voltage conditions for poling treatment

Thermal poling was done under air at normal pressure. The glass plates were heated at the poling temperature for at least one hour before applying an electric field during 30 min. Samples were previously cooled down to room temperature before removing the dc bias. At the anode, materials without ionic conduction (silicon, stainless steel) were used to avoid charges injection into the sample during the poling process. At the cathode, a sodalime glass was used as a non-blocking electrode which avoids the reduction of the sample at the cathode. Contacts between each electrode and the sample were carefully checked in order to preserve a good optical quality after the thermal poling treatment. Of course, these contacts are strongly dependent on the quality of the polishing on each side (anode and glass) of the glass plates.

For poling conditions optimization, preliminary electrical current measurements were performed during poling for five different applied constant voltages ranging from 0.5 to 3.5 kV. For each curve reported in Fig. 1, we measured periodically the electrical current during progressive heating of the glass plate at a rate of 10°C/mn until a current saturation due to the breakdown in the glass. These measurements performed at constant voltage indicate the range of temperatures where the ionic conductivity is optimum, and therefore the optimized poling conditions (voltage, temperature).

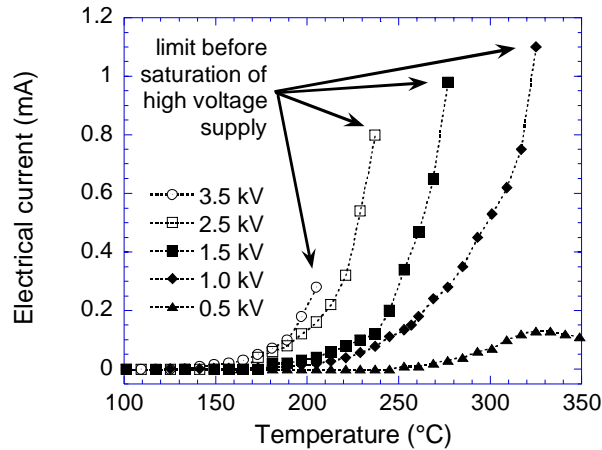


Fig. 1. Electrical current (in mA) as a function of temperature increase for several fixed external applied voltages (in kV).

Two experiments were performed for two sets of convenient optimized poling conditions (see Fig. 1) applied to glass samples namely S1 (S2) poled at 210°C (310°C) under 2.5 kV (1kV) during 30 min. Further SEM analysis of the anode surfaces of the glasses illustrated that the glass samples were not damaged during the poling process.

2.3. Optical characterization

Original second harmonic generation (SHG) measurements in both transmission and reflection modes were performed at 1064 nm. More details about the experimental setup and the analysis can be found elsewhere [5]. For the two samples, a typical energy of 150 μ J was necessary to record simultaneously the harmonic transmitted and reflected pp and sp polarized Maker-fringe patterns with a coupled θ -2 θ goniometer. The registered experimental patterns were found identical for S1 and S2, showing large SHG efficiencies, and were simulated as previously described. The linear refractive indices at 1064 nm ($n_{1064} = 1.91 \pm 0.02$) and 532 nm ($n_{532} = 1.99 \pm 0.02$) were previously measured, using the Brewster angle linear reflection method over the $\pm [10^\circ; 80^\circ]$ wide θ range, and used for the simulations. The coherence length for the NLO layers was calculated $L_c = \lambda / (4|n_{1064} - n_{532}|) = 2.95 \mu m$. For poled glasses without absorption, the contracted 3×6 SHG tensor contains two non-zero coefficients: $\chi_{33}^{(2)} = 2 \cdot d_{33}$ and $\chi_{31}^{(2)} = 2 \cdot d_{31}$. We assumed the SHG signal is due to a charge migration process during poling and in this case $d_{33} = 3 \cdot d_{31}$ is fixed for the simulation [1,2]. Experimental and simulated signals are given for S2 in Fig. 2.

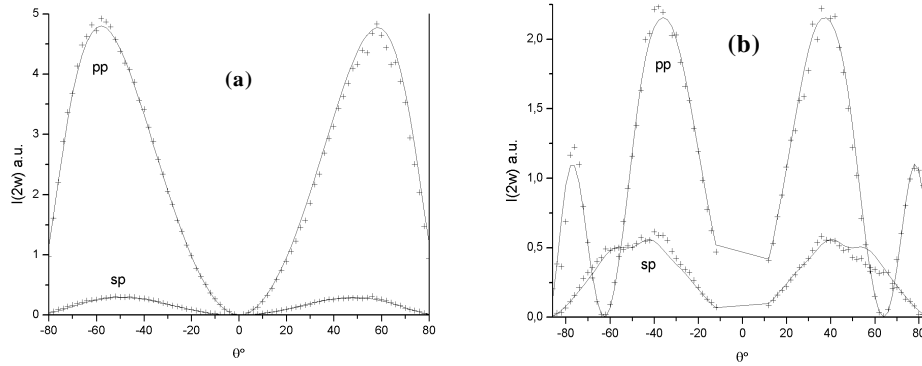


Fig. 2. Experimental (crosses) and calculated (solid lines) transmitted (a) and reflected (b) polarized Maker-fringe patterns of samples S2 poled 30 nm at 310°C with 1.0 kV. The polarized geometries *pp* and *sp* correspond to either a *p* (in plane) or *s* (out of plane) polarized incident beam, respectively, and a *p* polarized harmonic signal.

3. Results

The glass composition has been analyzed after elaboration and proved to be homogeneous from sample to sample (Na (11.5 ± 0.5 at %), Nb (15 ± 0.5 at %), P (8.5 ± 0.5 at %), O (65 ± 0.5 at %), Boron could not be detected). The discrepancies between the theoretical composition and the real value are identical for both S1 and S2.

The same NLO efficiencies were obtained for S1 and S2, which were poled under different poling conditions. For the Maker-fringe patterns simulations, we have first assumed that the nonlinear optical zone is buried under the anode [1, 2]. Then we introduced a d_{33} stepwise profile with three identical stepwidth layers. A final layer with $d_{33} = 0$ was added in the simulations for the remaining glass thickness. Only 4 parameters were therefore necessary to fit the four polarized experimental patterns: the total thickness of the three NLO layers and one constant d_{33} coefficient for each of the 3 NLO layers (the overall thickness of the glass being first measured and fixed for the simulations). The information contained in the reflected spectra allowed this elaborate and original profile simulation. Close to the anode surface, the d_{33} coefficient reaches a maximum value which is 10 times the quartz response (~ 2.5 pm/V), and the overall thickness of the nonlinear zone is estimated to be about $5 \mu\text{m}$.

4. Discussion

It can be noticed that even though S1 and S2 have been poled under different poling conditions, they both show the same NLO efficiencies. For these sodium rich glasses with large conductivity, the motion of charges under optimized stable conditions seems to be essential despite the chosen level of the external applied voltage.

The simulated $\chi^{(2)}$ NLO layer profile obtained from two independent experiments is reported in Fig. 3. As previously pointed out the information contained in both transmitted and reflected spectra allows to precisely simulate a more realistic profile compared to a one step profile usually simulated. The large $\chi^{(2)}$ susceptibilities which are obtained next to the anodic glass surface (about 10 times the quartz response) can be explained at first view by a migration process of sodium cations from the anode to the cathode during the poling process, involving the formation of a negative charged depletion zone under the anode [1, 2]. When removing the electrodes an internal field E_{int} remains buried inside the depletion zone and couples to the $\chi^{(3)}$ susceptibility of the glass to give: $\chi^{(2)} = 3 \cdot \chi^{(3)} \cdot E_{\text{int}}$ [1,2,6,9]. According to this charge migration model mechanism, the large ionic conductivity of our glasses is favourable to induce a complete screening of the field in the anodic nonlinear depletion zone.

On the other hand the large $\chi^{(3)}$ susceptibility due to the large concentration of niobium in the glass is a major factor to explain the generation of high level $\chi^{(2)}$ susceptibilities [7, 8].

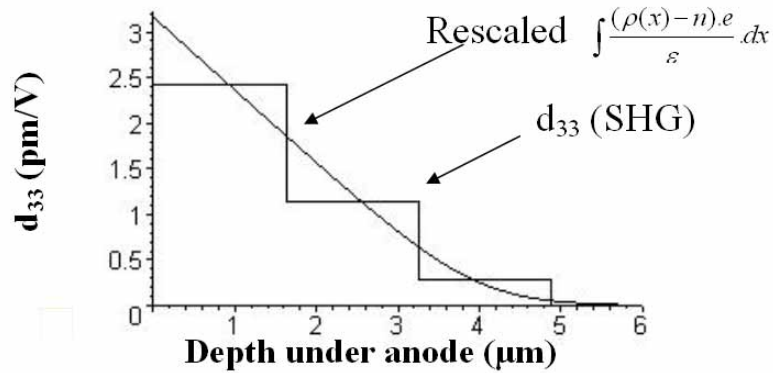


Fig. 3. Simulated d_{33} profile obtained for the sample (S2) obtained from the SHG patterns (stepwise profile). A comparison is furthermore given with a rescaled profile of the integrated Poisson's law deduced from the sodium depletion concentration of Fig. 4.

A correlation to the atomic concentration of sodium remaining in the NLO zone after poling has been tested through EDS analysis. The result obtained throughout the cross-section of the S2 poled glass from the anodic surface is presented in Fig. 4. The glass is surprisingly found to be completely depleted next to the surface and recovering a normal sodium concentration 5 μm under the surface for both S1 and S2 samples.

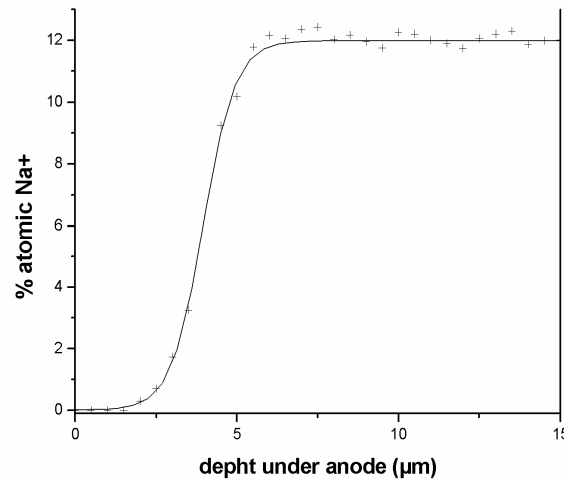


Fig. 4. Experimental (crosses) and smoothing (solid line) depth profiles of the atomic concentration of sodium in S2 from 0 μm (anode surface) to 15 μm inside the nonlinear and linear layers.

It is important to notice that if we consider sodium as the only mobile constituent involved in the depletion zone production we obtain a contradiction in calculating E_{int} within this simplistic hypothesis. By integrating the Poisson's Law $d(E_{\text{int}})/dx = (\rho(x)-n)e/\epsilon$, (where ϵ denotes the glass permittivity, e the elementary charge, $\rho(x)$ the profile of sodium

concentration, and n the negative charge concentration assumed to be constant), we effectively obtain an internal electric field E_{int} too large by 5 orders of magnitude, which should lead to the breakdown of the glass. Nevertheless, it is very tempting to emphasize the similarity between the NLO simulated profile and a rescaled integrated Poisson's law (Fig. 3) deduced from the sodium depletion profile measured by EDS (Fig. 4). More investigations have to be performed on such sodium rich glasses to elaborate a new model in accordance with these novel conductive glasses.

4. Conclusion

In conclusion, we provide in this work a pathway to control and optimize the thermal poling treatment of sodium rich borophosphate glasses. The linear $\chi^{(2)}$ profile of these poled glasses is determined through a novel combined analysis of transmitted and reflected polarized Maker-fringe patterns. All the experimental results tend to show that the non linearity is confined in a layer of 5 μm depth where $d_{33} = \sim 2.5 \text{ pm/V}$ ($\chi^{(2)} = \sim 5 \text{ pm/V}$) at the anode side. Such NLO efficiency opens up the possibility of future glassy active electro-optical devices fabrication.

Acknowledgments

V.R. and F. A. acknowledge the Région Aquitaine for SHG equipments.